A study of muon localization and diffusion in Hf_2Co and Hf_2CoH_3

1992 J. Phys.: Condens. Matter 4 5025

(http://iopscience.iop.org/0953-8984/4/21/018)

J. Phys.: Condens. Matter 4 (1992) 5025–5036. Printed in the UK

A study of muon localization and diffusion in Hf_2Co and Hf_2CoH_3

A Baudry†¶, P Boyer†*, L P Ferreira‡, S W Harris§, S Miraglia|| and L Pontonnier||

† Centre d'Etudes Nucléaires, DRFMC/SP2M/MP, 85X, 38041 Grenoble Cédex, France
‡ Departamento de Fisica, Universidade de Coimbra, 3000 Coimbra, Portugal
§ Uppsala University, Box 530, S-751 21 Uppsala, Sweden
|| Laboratoire de Cristallographie, CNRS, 166X, 38042 Grenoble Cédex, France

Received 3 December 1991, in final form 3 February 1992

Abstract. Muon spin relaxation (μSR) experiments were carried out in zero field on polycrystalline samples of Hf_2Co and Hf_2CoH_3. In the unhydrided alloy the muon preferentially occupies octahedral interstices and diffuses through a tunnelling mechanism within the network made of adjacent octahedra above 220 K. In contrast, the muon occupies tetrahedral interstices in the hydrided alloy. Muon diffusion takes place through two distinct phonon-assisted tunnelling mechanisms with a possible contribution of over-barrier hopping above 250 K, and appears to be strongly enhanced by the presence of hydrogen. This effect is attributed to the different pathways taken by the muon in hydrided and unhydrided Hf_2Co. A comparison with the hydrogen jump rate measured by perturbed angular correlation in the same hydride provides confirmation that the hydrogen mobility is indeed faster than that of the muon, which appears to be a quite general result in concentrated metallic hydrides.

1. Introduction

Hf_2Co belongs to the class of binary alloys formed between early and late transition metals, which have been recognized as interesting systems for hydrogen storage, especially in their amorphous phases (Harris *et al* 1987). Typically these alloys are able to form ternary hydrides corresponding to hydrogen-to-metal atom ratios $H/M \geqslant 1$ at rather low temperatures ($T \leqslant 300$ °C) under low hydrogen pressure.

The diffusional properties of hydrogen in highly concentrated hydrides of Zr_2Ni were recently studied with several techniques including ^1H nuclear magnetic resonance (NMR) (Aubertin *et al* 1987, 1989, 1990), ^{181}Ta spin relaxation measured by perturbed angular correlation (PAC) of gamma rays (Boyer and Baudry 1987, Baudry *et al* 1988, 1990a, Chikdene *et al* 1989) and muon spin relaxation (μSR) (Boyer and Baudry 1989, Baudry *et al* 1990b). In the polycrystalline hydrides Zr_2NiH_x very good agreement was found between ^1H NMR and ^{181}Ta PAC data. These results can be reasonably understood within a rather crude elastic model based on the crystallographic data yielded by neutron diffraction (Chikdene 1989). The μSR experiments

¶ Also affiliated to the CNRS.
* Also affiliated to Université Joseph Fourier, Grenoble.

0953-8984/92/215025+12$04.50

performed on the same materials have revealed that the motion of the positive muon relative to the protons is apparently significantly slower than the hydrogen motion as observed in PAC or NMR experiments (Baudry *et al* 1990b). A similar 'slowing-down' effect was found in several metallic hydrides (Gygax *et al* 1984, Kossler *et al* 1986, Kempton *et al* 1989), including the Laves phase hydrides ZrV_2H_x in which the muon diffusion is measured with respect to the stiff host metal lattice because the contribution of the protons to the depolarization of the muon is small (Hempelmann *et al* 1989). Qualitatively this effect suggests that either the hopping rate of the protons is affected by the presence of the muon or that the muon hops slower than a proton, or both. Recent numerical simulations based on Monte Carlo calculations support the existence of such a perturbation in the dynamics of the muon–proton system (Kempton *et al* 1989). However, the underlying mechanism giving rise to this surprising effect remains somewhat mysterious. Unfortunately, no comparison with the diffusive motion of the solitary muon in Zr_2Ni could be made as the nuclear moments of the metal atoms are very small.

More recently, an investigation of Hf_2Co hydrides was initiated with the PAC and μSR techniques. Hf_2Co displays a cubic, Ti_2Ni-type structure belonging to the $Fd3m$ space group with $a = 12.071$ Å (Van Essen and Buschow 1979). The interstitial positions available to hydrogen atoms or positive muon are shown in figures 1–3. Following the notation introduced by Westlake (Westlake 1983), six sites D_n ($1 \leqslant n \leqslant 6$) with tetrahedral coordination and two octahedral sites, O_1 and O_2, are distinguished. The D_1(32e) and D_3(96g) sites correspond to an $(Hf1)_3$–Co coordination with equivalent Hf1 atoms. Two types of inequivalent Hf atoms enter the coordination $(Hf1)_2$–Hf2–Co of D_2(192i) sites. The D_4(96g) site is Hf1–Hf2–$(Co)_2$ coordinated. The D_5 and D_6 sites present a Co-rich coordination, Hf2–$(Co)_3$ and $(Co)_4$ respectively, and their occupation is very unlikely. Both the octahedral sites are surrounded by six Hf atoms. As a remarkable feature of this structure we observe that D_1 and D_3 sites share a face with adjacent O_1(8a) and O_2(16c) sites respectively. Adjacent O_1 and O_2 sites have a shared face as well.

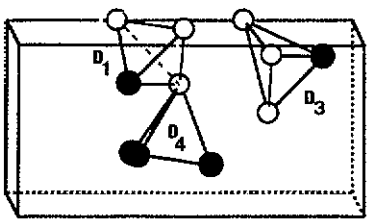

Figure 1. A fundamental building block (one-quarter of the unit cell) of the cubic Ti_2Ni-type structure of Hf_2Co, showing only three types of tetrahedral interstices. Non-equivalent Hf1 (48f positions) and Hf2 (16d positions) atoms are represented by white and 'grey' circles respectively, and cobalt atoms (32e positions) by black circles.

No determination of the site occupancies in $Hf_2CoH(D)_x$ exists presently. However, neutron diffraction data are available for the isostructural hydrides Hf_2FeH_x (Soubeyroux *et al* 1987). For $x \simeq 3$, the largest fraction ($\sim$ 80%) of the hydrogen (deuterium) atoms is accommodated in tetrahedral D_3 sites, the rest being localized in T_1(32e) sites with the $(Hf1)_3$ triangular coordination. The authors do not exclude the presence of a small amount ($\simeq$ 5%) of hydrogen in other interstitial sites. When the concentration of hydrogen is increased ($x \simeq 4$), the D_2 and D_4 sites become

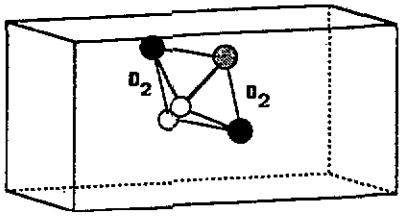

Figure 2. A fundamental building block of Hf_2Co showing only two adjacent D_2 tetrahedral sites. Circles as in figure 1.

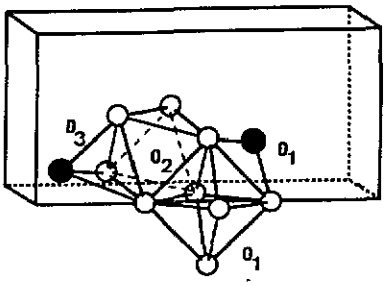

Figure 3. Arrangement of two adjacent octahedral interstices $O_1(8a)$ and $O_2(16c)$. Two tetrahedra D_1 and D_3 sharing a face with the O_1 and O_2 octahedra respectively are also shown. Circles as in figure 1.

significantly populated. This filling scheme obeys chemical and geometrical criteria such as the difference in the chemical attraction of the host atoms, the hole size and the minimum H–H distance. Although the same criteria are favourable for the occupation of the octahedral sites, these actually remain unoccupied (Soubeyroux *et al* 1987).

In this article are presented the results of zero-field μSR experiments conducted on polycrystalline Hf_2Co and the hydride Hf_2CoH_3. The μSR data are compared with the PAC data obtained for the hydrided alloy.

2. Experimental details

Polycrystalline Hf_2Co was prepared from high purity hafnium (99.9 with $\sim 2\%$ Zr) and cobalt (99.99) by HF melting under 5N argon atmosphere. The alloy was then heated for 10 days at 800 °C under inert atmosphere. The recorded x-ray diffraction pattern was as expected for a cubic Ti_2Ni-type structure, no additional lines could be clearly distinguished. However, electron microscopy pictures revealed the existence of small hafnium-rich zones. PAC measurements using the ^{181}Ta probe supported the electron microscopy data: in addition to the two anticipated components with amplitudes in the ratio 1:3, corresponding to the quadrupole couplings at the two distinct Hf(Ta) sites of the Ti_2Ni-type structure, a third weak component ($\simeq 10\%$) should be introduced in order closely to reproduce the measured quadrupole spectrum. The hydride Hf_2CoH_3 was produced by exposing the alloy to a low hydrogen pressure ($\leqslant 10^5$ Pa) at 350 °C. Prior to hydrogenation the alloy was heated for several hours at 550 °C under high vacuum. X-ray diffraction showed narrow lines corresponding to the cubic structure of the alloy with $a = 10.744$ Å. This value corresponds to a

relative expansion of the unit cell volume of $\sim 18\%$. In isostructural Hf_2FeH_3 the volume expansion is only $\sim 13\%$ (Soubeyroux *et al* 1987).

Muon spin relaxation measurements were made in zero field using the ISIS pulsed muon source of the Rutherford Appleton Laboratory. This set-up has the greatest sensitivity to slow dynamics, as slow diffusion manifests itself only as a change in the value of the depolarization rate in measurements in an applied transverse field, whereas in zero field, the actual shape of the time spectra is modified. Large samples (35 mm diameter) were used in order to minimize the background component corresponding to the muons stopped outside the sample to below 20% of the total amplitude. This background component was measured separately with an $ErAl_2$ reference sample under identical experimental conditions. Zero-field measurements require careful normalization to account for the difference between detector efficiencies in backward and forward directions. The normalization coefficient was determined from a transverse-field measurement ($B = 20$ G) on $ErAl_2$ as explained in a recent paper by Dalmas de Réotier and co-workers (Dalmas de Réotier *et al* 1990).

3. Results and discussion

The results of the measurements on the unhydrided and hydrided samples are presented separately. The discussion includes a comparison with the results obtained from PAC in the same hydride.

3.1. Hf_2Co

Typical zero-field spectra measured at different temperatures are shown in figure 4. From the shape of the spectra two temperature ranges can be clearly distinguished. Below about 200 K it appears that the muon does not thermalize in a single interstitial site. On the other hand, the shape of the spectra recorded above 200 K suggests rather that the muon diffuses through identical sites. To examine the behaviour of the muon quantitatively with temperature, a fit has been carried out to all the spectra using the expression for the depolarization factor given by the 'strong collision' approximation:

$$G(t) = G(0,t)\exp(-\nu_d t) + \nu_d \int_0^t G(\nu_d, t'-t)\exp(-\nu_d t)G(0,t')\,dt'. \qquad (1)$$

In the expression above ν_d is the correlation frequency characteristic of the fluctuations of the dipolar interaction between the diffusing muon and the surrounding nuclear moments. The static depolarization function $G(0,t)$ has been assumed to be properly described by the Kubo–Toyabe formula (Hayano *et al* 1979) derived for an isotropic Gaussian distribution of local fields:

$$G(0,t) = \tfrac{1}{3} + \tfrac{2}{3}(1-\Delta^2 t^2)\exp(-\Delta^2 t^2/2). \qquad (2)$$

Below 220 K, the spectra are well represented by a fit with two superimposed depolarization functions (and a constant background) characterized by quite different distributions of static fields. This clearly indicates that the thermalized muon lies in two different sites. At 30 K the amplitudes of the two components contributing to the depolarization factor are equal within the experimental error. The widths of the Gaussian distributions of static fields are $\Delta_1 = 0.080(3)$ MHz and $\Delta_2 = 0.420(7)$ MHz

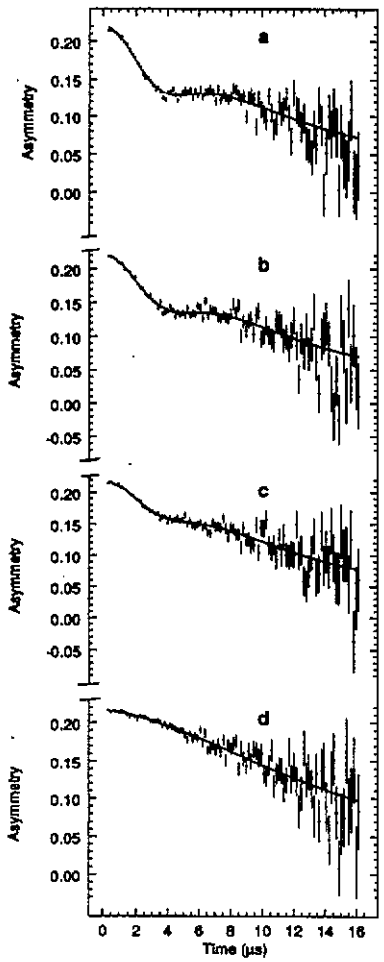

Figure 4. Asymmetry of the disintegration of the positive muon measured in zero field in Hf_2Co at different temperatures: (*a*) 30 K, (*b*) 130 K, (*c*) 180 K and (*d*) 240 K. In (*a*), (*b*) and (*c*) the full curve is the result of fitting to the sum of two Kubo–Toyabe functions (equation (2)). At 240 K, the data are fitted to a single Gaussian–Markovian function (equation (1)).

respectively. The temperature dependence of the amplitudes of the two depolarizing components is shown in figure 5. The amplitude a_2 of the second component (site 2) is found to decrease continuously above 50 K until it disappears by 250 K. The amplitude a_1 corresponding to muons thermalized in site 1 increases simultaneously, and the full asymmetry maintains a constant value of $\simeq 0.185$ (excluding the amplitude of the background component, which was fixed at 0.03 at all temperatures). Above 250 K the depolarization function is well fitted to a single function given by equation (1) including a static field distribution with $\Delta = 0.08$ MHz. It is worth noting that the spectra do not reveal any significant dynamic contribution to the muon depolarization below 200 K. These results strongly suggest that site 2 depopulates into site 1 without long-range diffusion of the muon. This is possible if the sites 1 and 2 are in first-neighbour positions, in such a way that a thermalized muon in site 2 can reach site 1 after a single 'jump'. However, the temperature dependence of the

populations of the two sites as displayed in figure 5 is not fully consistent with a two-state reaction process controlled by a jump rate obeying an Arrhenius law. A lower activation energy can be actually anticipated for muon hops from site 1 into site 2 as the temperature rises because of the increasing population of higher vibrational levels of the muon and the correlated lowering of the apparent potential barrier due to a higher tunnelling rate. Nevertheless, from the data below 180 K a maximum value of this energy can be roughly estimated at ~ 30 meV, assuming that the amplitudes measured for the two distinct depolarization functions at a given temperature are averaged values over the time window characteristic for our experiment, i.e. $\sim 10^{-5}$ s. A more exact procedure should require the introduction of time-dependent amplitudes in the depolarization functions in order to take into account the depopulation of site 1 into site 2.

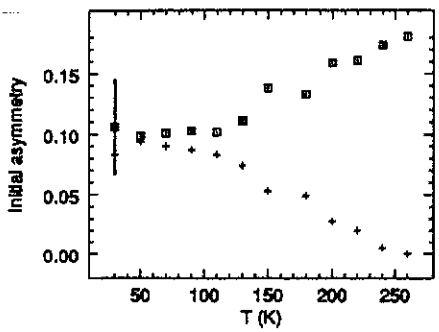

Figure 5. Temperature dependence of the asymmetries a_1 (□) and a_2 (+) corresponding to the two fractions of muons observed below 240 K in Hf_2Co.

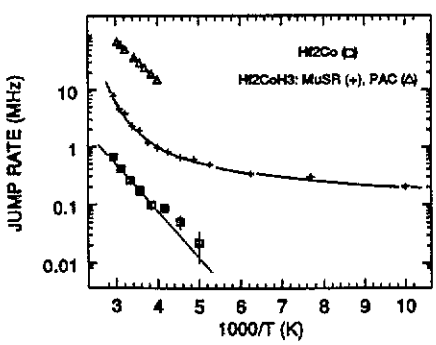

Figure 6. Arrhenius plots of the muon jump rate in Hf_2Co (□) and Hf_2CoH_3 (+). The values of the hydrogen jump rate measured by PAC on the Hf-substitutional ^{181}Ta probe in Hf_2CoH_3 (Δ) are also shown for comparison.

The parameter Δ of the static depolarization function in zero-field experiments can be calculated at each interstitial site available to the muon within the Van Vleck approximation for non-identical spins (Van Vleck 1948). The results of such calculations applied to Hf_2Co taking into account the nuclear moments over a distance of 70 Å around the position of the interstitial muon are reported in table 1. Cobalt consists of 100% ^{59}Co with a nuclear moment of $4.58\mu_N$ whereas most of the natural hafnium isotopes are non-magnetic except ^{177}Hf with 18.6% abundance and a

nuclear moment of $0.61\mu_N$, and ^{179}Hf with 13.7% abundance and a nuclear moment of $0.47\mu_N$ (Lederer *et al* 1967). The contribution of Hf nuclei to the static depolarization of the muon in octahedral positions can be estimated at $\sim 8\%$, and is still lower when the muon lies in tetrahedral sites. Therefore the contribution of Hf nuclei was reasonably neglected in our calculations. An expansion of 5% of the lattice parameter was assumed in order to take into account the small-polaron effect which pushes the surrounding metal atoms aside. This effect reduces the values of Δ by $\simeq 13\%$ for the tetrahedral sites and $\simeq 18\%$ for the octahedral sites. By comparing the calculated values of Δ to the experimental results, the muon sites 1 and 2 may be unambiguously identified with octahedral and tetrahedral D_1, D_2 or D_3 sites respectively. This site assignment could be reasonably anticipated from the nature of the nearest-neighbour atoms, which contribute predominantly to the dipole interaction with muons in the different interstitial positions: in the octahedral sites the muon is surrounded by six non-magnetic Hf atoms whereas it has one magnetic Co atom as nearest neighbour in the tetrahedral sites. Let us note the close agreement between the calculated and measured values of Δ relative to the tetrahedral positions while the value calculated for the octahedral positions is about 20% higher than the measured value. Maybe this is an indication that the polaron effect is stronger when the muon is located in octahedral positions. Furthermore we should realize that the Van Vleck approximation does not take into account the existence of electric field gradients, which change the nuclear dipole fields (Hartmann 1977).

Table 1. Width of the distribution of static dipolar fields (Δ_{calc}) calculated at the different interstitial positions available to the thermalized muon in Hf_2Co. Δ_1 and Δ_2 are the widths of the field distributions characteristic of the two distinct muon sites observed below 240 K. Above 240 K only the single distribution Δ_1 is observed.

Interstitial site		Δ_{calc} (MHz)	Δ_1 (MHz)	Δ_2 (MHz)
Tetrahedral	D_1(32e)	0.422		0.420(7)
	D_2(192i)	0.421		
	D_3(96g)	0.421		
	D_4(96g)	0.509		
Octahedral	O_1(8a)	0.097	0.080(3)	
	O_2(16c)	0.101		

As the values of the parameter Δ calculated for the different tetrahedral sites are very close, nothing may be claimed regarding the probability that each of them is occupied by the thermalized muon. The same remark hold for octahedral sites. Let us note, however, that muons located in D_1 or D_3 holes can easily go through the face shared with the adjacent O_1 and O_2 octahedra respectively. However, these easy jump paths do not exist for the muons thermalized in D_2 tetrahedra, which share only vertices with neighbouring octahedra (see figures 1–3). The quite small value ($\leqslant 30$ meV) estimated for the activation energy that controls the muon jump suggests that the former situation with 50% of the muons thermalizing in D_1 and/or D_3 sites is more likely.

Above 220 K, the thermalized muon occupies octahedral sites. In agreement with the time dependence of the depolarization factor, the muon diffuses within the three-dimensional array formed by octahedral sites. The most likely diffusion pathway goes

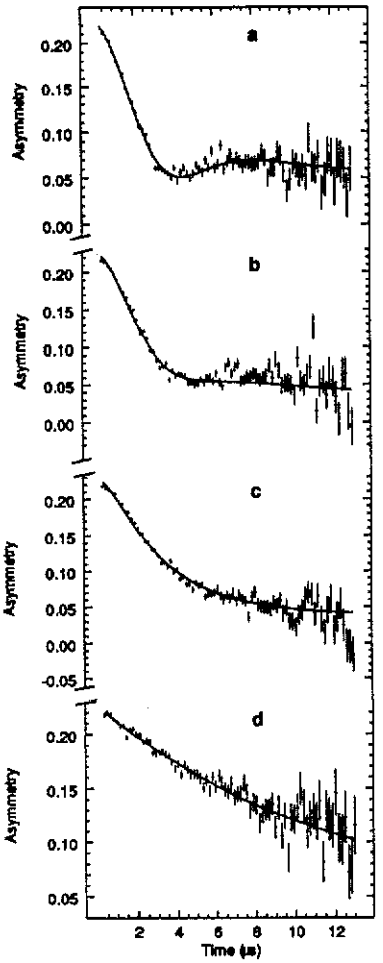

Figure 7. Examples of asymmetry functions of the positive muon implanted in Hf_2CoH_3 at different temperatures: (*a*) 30 K, (*b*) 160 K, (*c*) 250 K and (*d*) 325 K. The full curves are the results of fitting to equation (1).

through the face shared by adjacent O_1 and O_2 octahedra. The Arrhenius plot of the frequency ν_d of the dipolar fluctuations induced by muon diffusion is shown in figure 6. The experimental values are well fitted to the following expression:

$$\nu_d = 4.5(3) \times 10^8 \exp[-0.190(5)\ \text{eV}/kT]\ \text{s}^{-1}.$$

The small value of the pre-exponential term is consistent with diffusional motion dominated by a phonon-assisted tunnelling mechanism. On the other hand, the rather high value of the activation energy ($\sim$ 0.2 eV) involved in this tunnelling process implies that the potential barrier the muon must overcome in a classical over-barrier jump between adjacent octahedral sites is higher than 0.5 eV. This value is the result of a rough estimation assuming the over-barrier jump frequency is only $\sim$ 1% of the tunnelling frequency at 300 K, and anticipating a pre-exponential factor for over-barrier jumps in the range 10^{11}–10^{12} s^{-1} in agreement with the values observed in several hydrided alloys (Harris 1991).

3.2. Hf_2CoH_3

In comparison with the unhydrided alloy, the situation appears more straightforward in the hydride. Examples of depolarization factors measured in Hf_2CoH_3 are shown in figure 7. The experimental data are well-fitted to the theoretical function (1) with $\Delta = 0.440(5)$ MHz throughout the temperatures investigated. Reference to table 1 shows that this value is in accordance with muons localized in tetrahedral sites. This result is consistent with the interstitial site occupancies determined from neutron diffraction data in Hf_2FeH_3. Let us remember that in this hydride the octahedral holes are empty, the H atoms being localized in either tetrahedral D_3 (80%) or triangular T_1 (20%) sites (Soubeyroux *et al* 1987). The occupation of octahedral holes by the muon is therefore hindered by the presence of hydrogen.

The Arrhenius plot of the correlation frequency of the dipolar fluctuations is shown in figure 6. It clearly appears that the diffusing motion of the muon does not obey a single Arrhenius process but rather results from the superposition of at least two distinct processes, which coexist at high temperatures as indicated by the smooth transition in the slope of the Arrhenius plot. Actually the temperature dependence of the correlation frequency is properly reproduced by the sum of two Arrhenius functions given by the following expressions:

$$\nu_d^1 = 3.2(3) \times 10^6 \exp[-0.032(8)\ \mathrm{eV}/kT]\ \mathrm{s}^{-1}$$
$$\nu_d^2 = 4.6(1) \times 10^{10} \exp[-0.26(2)\ \mathrm{eV}/kT]\ \mathrm{s}^{-1}.$$

The fit is significantly improved when a small temperature-independent component corresponding to a correlation frequency of ~ 0.14 MHz is included in the fitting procedure. Such a flat component with a similar correlation frequency was observed in hydrides of Zr_2Ni (Baudry *et al* 1990b). Its origin is not understood; however, it is worth noting that the static limit as described by equation (2) is not reached at 30 K. Possibly some relationship exists between the 'residual' dynamical effects observed at very low temperatures and spin dynamics phenomena that are not taken into account in the Kubo–Toyabe depolarization function (Dalmas de Reotier *et al* 1992). For a more complete description of the depolarization factor, a quantum-mechanical treatment of the interactions would be required.

The first Arrhenius process (ν_d^1), which dominates below 250 K, is determined by parameters typical of a phonon-assisted tunnelling motion. Above 250 K, some contribution of over-barrier hopping to the muon diffusion cannot be excluded, in accordance with the expression of the correlation frequency ν_d^2. A qualitatively similar behaviour of the muon has been observed in amorphous Zr_2NiH_4 (Baudry *et al* 1990b). On the other hand, in contrast with the present result, the muon diffusion measured in the crystalline hydrides of Zr_2Ni has been found to obey a single Arrhenius law characteristic of an over-barrier hopping process (Baudry *et al* 1990b).

One of the definite advantages of μSR spectroscopy over the other available microscopic techniques is its ability to provide unique information regarding the localization of both the single muon and the muon in the presence of hydrogen. The accommodation of the solitary muon in octahedral sites in unhydrided Hf_2Co appears to be in contrast with the occupation of tetrahedral sites in the hydrided sample as anticipated from the occupancy rates determined in the concentrated hydrides of Hf_2Fe and confirmed by μSR data analysis. On the other hand, the occupation of octahedral sites is consistent with minimum size and chemical affinity criteria. Finally,

the different localization of the muon in unhydrided and hydrided Hf_2Co gives direct evidence that the filling process of the interstitial sites by hydrogen is accurately controlled by H–H interactions.

Figure 6 allows a comparison of the Arrhenius plots of the correlation frequencies measured in unhydrided and hydrided Hf_2Co to be made. The muon diffusion appears to be strongly modified by the presence of interstitial hydrogen. Above 200 K the diffusional motion of the single muon in the unhydrided alloy is controlled by quantum tunnelling effects while the muon traces the hydrogen motion and moves by crossing over a significantly higher potential barrier in the hydride. Somewhat atonishing is the lower derived jump rate for the single muon than for the muon–hydrogen correlated motion. It appears that the presence of hydrogen leads to an enhancement of the muon diffusion by an order of magnitude. A similar, but less pronounced, effect has been observed recently in amorphous CuTi (Harris *et al* 1991, Harris 1991). The authors have noted that such an effect is in contradiction with the concept of hydrogen blocking the motion, and argued that hydrogen must expand the lattice, permitting a more facile muon motion. However, in the case of Hf_2Co the interstitial sites visited by the diffusing muon are different in the unhydrided alloy and the hydride. Therefore, the hydrogen-induced enhancement of the muon jump rate is most likely related to distinct diffusion pathways taken by the muon in both samples. The muon–proton interaction prevents muon diffusion through octahedral holes. Moreover, the site and saddle-point energies of the different sites are modified by the presence of hydrogen. Let us add that these observations prompt us to believe that distinct diffusion pathways could exist for the muon in unhydrided and hydrided amorphous CuTi.

In figure 6 the data obtained from preliminary PAC experiments using ^{181}Ta as a substitutional quadrupole probe are also reported for the hydride Hf_2CoH_3. In a PAC experiment the jump rate of the mobile protons is deduced from the quadrupole relaxation measured at the Hf(Ta) sites. As previously reported for several systems such as titanium hydrides (Kempton *et al* 1989), the Laves phase hydrides ZrV_2H_x (Hempelmann *et al* 1989) and the hydrides of Zr_2Ni (Baudry *et al* 1990b), the muon appears to diffuse more slowly than hydrogen in Hf_2CoH_3. The activation energies that control the muon and proton diffusion at high temperatures are very close, 0.26 eV and 0.24 eV respectively. This indicates that the muon traces the hydrogen. The existence of a rather broad distribution around the mean value $\langle E_a \rangle = 0.24(2)$ eV revealed by PAC measurements should be mentioned. The muon slowing down corresponds therefore to a drop in the prefactor of the Arrhenius law. This suggests that the origin of this paradoxical effect is in some way connected with a change in the muon vibrational states in the proximity of protons. Localized vibrational states of the muon are, to some extent, coupled with the collective modes of hydrogen, which are themselves perturbed by the presence of the lighter muon. The larger size of the local distortion created around the muon (small-polaron effect) possibly contributes to this phenomenon. On the other hand, this effect could partly originate from the perturbation caused by the muon itself occupying a normally empty interstice and then 'blocking' the motion of neighbouring protons. Let us mention here that the remarkable reversed isotope effect such that heavier deuterons may diffuse faster than protons in Pd or Cu has been satisfactorily explained by computing the zero-point energy of the diffusing particle in the confining potential well perpendicular to the interstitial diffusion channel at the saddle point (Fujita and Garcia 1991). From the experimental point of view, μSR measurements in hydrided Hf_2Co at lower hydrogen

concentrations could help to understand the influence of muon–proton interactions on diffusion.

4. Conclusions

The work presented in this paper is one among the few studies of muon diffusional properties in intermetallic alloys and hydrides. Hf_2Co offers a beautiful illustration of the potential of μSR spectroscopy in this field. Of special interest is the unique possibility offered by this technique to determine the behaviour of the solitary muon in the metal host lattice. Marked differences have been seen in the localization and diffusion properties of the muon in the alloy and the hydride Hf_2CoH_3. In unhydrided Hf_2Co below 220 K the muons are separated into two distinct populations occupying tetrahedral and octahedral sites respectively. At higher temperatures, all the muons thermalize in octahedral sites and diffuse rather slowly through a tunnelling mechanism within the network of these octahedral holes.

The much faster diffusion observed in hydrided Hf_2Co corresponds to a different path taken by the muon within the network of the tetrahedral interstices. As evidence that the muon traces hydrogen we note the closeness of the activation energies of the muon and proton jump rates in the hydride at high temperatures. However, the dipolar correlation frequency characteristic of muon diffusion lies about an order of magnitude below the jump frequency measured by PAC for hydrogen. In this respect, the two hydrides Hf_2CoH_x and ZrV_2H_x in which the muon diffusion is measured with respect to the host metal network display quite similar behaviour. Such a hydrogen-induced slowing down of the muon diffusion compared with the proton appears to be a widely observed effect in metallic hydrides. Our feeling is that the answer to this open problem lies in the vibrational dynamics of the system made up of the muon and the surrounding hydrogen atoms.

References

Aubertin F, Campbell S J, Pope J M and Gonser U 1987 *J. Less-Common Met.* **129** 297–303

—— 1989 *Proc. VIIIth Int. Conf. on Hyperfine Interactions (Prague)*

—— 1990 *Hyperfine Interact.* **60** 817–20

Baudry A, Boyer P and Chikdene A 1988 *J. Less-Common Met.* **143** 143–50

—— 1990a *J. Phys.: Condens. Matter* **2** 8075–82

Baudry A, Boyer P, Chikdene A, Harris S W and Cox S F J 1990b *Hyperfine Interact.* **64** 657–64

Boyer P and Baudry A 1987 *J. Less-Common Met.* **129** 213–19

—— 1989 *IOP Short Meetings Series 22* (Bristol: IOP) pp 65–72

Chikdene A 1989 *Thesis* Université Joseph Fourier, Grenoble

Chikdene A, Baudry A and Boyer P 1989 *Z. Phys. Chem. NF* **163** 443–8

Dalmas de Réotier P, Yaouanc A and Meshkov S V 1992 *Phys. Lett.* **162A** 206–12

Dalmas de Réotier P, Yaouanc A, Eaton G H and Scott C A 1990 *Hyperfine Interact.* **65** 1113–6

Fujita S and Garcia A 1991 *J. Phys. Chem. Solids* **52** 351–5

Gygax F N, Hintermann A, Rüegg W, Schenck A, Studer W, Van der Wal A J, Stucki F and Schlapbach L 1984 *J. Less-Common Met.* **101** 327

Harris J H, Curtin W A and Tenhover M A 1987 *Phys. Rev.* B **36** 5784–97

Harris S W 1991 *Thesis* Uppsala University

Harris S W, Hartmann O, Wäppling R, Hempelmann R, Fell H-J, Scott C A and Maeland A J 1991 *J. Alloys Compounds* submitted

Hartmann O 1977 *Phys. Rev. Lett.* **39** 832

Hayano R S, Uemura Y J, Imazato J, Nishida N, Yamazaki T and Kubo R 1979 *Phys. Rev.* B **20** 850–9

Hempelmann R, Richter D, Hartmann O, Karlsson E and Wäppling R 1989 *J. Chem. Phys.* **90** 1935–49
Kempton J R, Petzinger K G, Kossler W J, Schone H E and Stronach C E 1989 *Phys. Rev.* B **40** 59–64
Kossler W J, Schone H E, Petzinger K, Hitti B, Kempton J R, Seymour E F-W, Stronach C E, Lankford W F and Reilly J J 1986 *Hyperfine Interact.* **31** 235
Lederer C M, Hollander J M and Perlman I 1967 *Tables of Isotopes* 6th edn (New York: Wiley)
Soubeyroux J-L, Fruchart D, Derdour S, Vulliet P and Rouault A 1987 *J. Less-Common Met.* **129** 187–95
Van Essen R M and Buschow K H J 1979 *J. Less-Common Met.* **64** 277–84
Van Vleck J H 1948 *Phys. Rev.* **74** 1168
Westlake D G 1983 *J. Chem. Phys.* **79** 4532